DTU Library

Magnetocaloric effect and H gradient in bulk La(Fe,Si)13Hy magnetic refrigerants obtained by HDSH

Neves Bez, Henrique; Eggert, Bruno G.F.; Lozano, Jaime; Bahl, Christian R.H.; Barbosa Jr., Jader R. ; Teixeira, Cristiano S. ; Wendhausen, Paulo A. P.

[Link back to DTU Orbit](#)

Magnetocaloric effect and H gradient in bulk La(Fe,Si)$_{13}$H$_y$ magnetic refrigerants obtained by HDSH

Henrique N. Bez[a,b,*], Bruno G. F. Eggert[a], Jaime A. Lozano[a], Christian R. H. Bahl[b], Jader R. Barbosa Jr.[a], Cristiano S. Teixeira[c], Paulo A. P. Wendhausen[a]

[a]*Mechanical Engineering Department - Federal University of Santa Catarina - Florianópolis, SC, 88040-900 - Brazil*
[b]*Department of Energy Conversion and Storage, Technical University of Denmark - Frederiksborgvej 399, DK-4000 Roskilde - Denmark*
[c]*Department of Engineering, Materials Engineering, Federal University of Santa Catarina - 89065-300 - Blumenau - Brazil*

Abstract

Results are reported on the preparation of bulk parts of La(Fe,Si)$_{13}$H$_y$ via the Hydrogen-Decrepitation-Sintering-Hydrogenation (HDSH) process. Net shape parts for application in room-temperature magnetic refrigeration have been produced in only 8 h of heat treatment which is considerably faster than the conventional ingot homogenization heat treatment of 7 days. The samples produced by HDSH showed higher amounts of hydrogen than the parts hydrogenated by the conventional method of thermal homogenization (20 h at 1423 K), milling to fine powder and subsequent hydrogenation. Hydrogenation parameters play an important role for the stability of the desired La(Fe,Si)$_{13}$ phase during the process. Hydrogen desorption was seen to occur at two temperature ranges as a result of internal grdients. Dissimilar amounts of α-Fe were precipitated for different hydrogenation times. As a result, parts produced via HDSH with 2 and 4 h of hydrogenation exhibited different magnetocaloric behaviours. For a hydrogenation step of 4 h, parts with a demagnetization factor of 0.49 showed an adiabatic temperature change (ΔT_{ad}) higher than 1 K for a temperature range of 40 K with a maximum value of 1.57 K for an applied magnetic field of 1.75 T. As the duration of the hydrogenation step of the HDSH process decreased to

---

*Corresponding author
Email address: hnbe@dtu.dk (Henrique N. Bez)

2 h, ΔT_{ad} was larger than 1 K for a temperature range of 24 K. However the maximum value of ΔT_{ad} at 328 K was 2.2 K, which is 37.5 % larger than the maximum value for a hydrogenation period of 4 h.

1. Introduction

The magnetocaloric effect (MCE) is the thermal response of certain materials when subjected to a changing magnetic field. It has been investigated since the early 19th century [1] and the pioneering work of Giauque and MacDougall [2] on ⁵ the use of adiabatic magnetization to cool below 1 K was awarded Nobel Prize in Chemistry in 1949. Magnetic refrigeration at room temperature was firstly demonstrated with gadolinium (Gd) as the magnetocaloric material, where a no-load temperature span of 47 K was achieved with approximately 157 g of Gd and a magnetic field of 7 T [3].

¹⁰ Magnetic refrigeration has a great potential for high thermodynamic cycle efficiency due to the reversible nature of the MCE [3, 4, 5]. The discovery of the giant MCE in Gd$_5$Si$_2$Ge$_2$ by Pecharsky and Gschneidner [6] prompted the research for other first-order phase transition (FOPT) materials with similar characteristics [7].

¹⁵ A more recent group of materials with promising properties is the La-based alloys, LaFe$_{13-x}$Si$_x$, which crystallise in the NaZn$_{13}$-type phase structure for values of x between 1.05 and 2.5 [8, 9]. Usually materials based on this phase are produced by a conventional melting, casting and annealing. The latter is necessary in order to achieve nearly 100 % of the desired phase and it is a long-²⁰ term homogenization step, which may take up seven days in high temperature heat treatments [10]. Faster routes have been proposed, e.g. melt-spinning, for which a nearly monophasic microstructure has been stabilised after a 2 h high-temperature heat treatment [11]. Other routes based on powder metallurgy have been suggested [12, 13].

2

LaFe$_{13-x}$Si$_x$ compounds have Curie temperatures, T_C, between 180 and 230 K, for increasing amounts of Si [14]. Therefore, to use this material for magnetic cooling around room temperature, the T_C must be increased. One possible method to increase the T_C of this material is by expanding the lattice parameter, e.g. inserting interstitial atoms such as H or C [15, 16]. The hydrogenation step is commonly performed in the powder form [17]. Nevertheless, after the hydrogenation process, where the hydrogen is inserted interstitially into the NaZn$_{13}$-type structure, some difficulties may be pointed out. Firstly, the resulting powder cannot be heat treated in order to shape it, since the hydrogen stability in the microstructure goes only up to around 500 K [16]. If one try to sinter under H$_2$ atmosphere, at around 1023 K LaH$_2$ starts to stabilize, destroying the desired phase. Hence, without being able to shape it, its application is now limited since in many cases a functional part with well-defined geometry is demanded [18].

In this work, the recently reported [19] Hydrogen-Decrepitation-Sintering-Hydrogenation (HDSH) process was used to produce bulk parts of La(Fe,Si)$_{13}$H$_y$, varying the H content in order to cover a broader range of working temperatures. Samples from the same ingot were also produced by the conventional process and the resulting samples from both processes were then compared.

2. Experimental Procedure

Bulk parts of La(Fe,Si)$_{13}$H$_y$ were produced by HDSH, as described in previous work [19]. The process is divided in 3 basic steps:

1 The process uses a La-Fe-Si ingot as raw material, which is hydrogen-decrepitated into small pieces, at 423 K during 1 hour.

2 The material is then milled, pressed into 1 mm thick pellets and sintered at 1423 K, for 6 h under argon atmosphere. During the heating step of the sintering, the hydrogen that was inserted in the material during HD is desorbed due to the high temperatures.

3

3 In the cooling step after the sintering, the temperature is reduced to 773 K and the hydrogenation step is, thus, performed during two different time spans: 2 and 4 h; under pure H_2 atmosphere at pressures above 1 atm. In this step the interconnected pores are the free path for hydrogen, so it may reach the whole sample volume. Subsequently, the samples are slowly cooled to room-temperature in the furnace.

In order to compare and evaluate the HDSH process, $La(Fe,Si)_{13}H_y$ powder was prepared by the conventional method, which is divided in 3 basic steps:

1 Cylindrical parts of the same ingot used to produce the HDSH parts, were cut by electro-erosion.

2 The parts were homogenized during 20 h at 1423 K under a 90 kPa Ar atmosphere.

3 The parts were then milled into powder ($<100 \ \mu m$) and a hydrogenation step was carried out, for 2 h at 773 K under pure H_2 atmosphere at pressures above 1 atm.

The phase constitution of the samples was determined via means of powder X-ray diffraction (XRD) on a Phillips X'Pert Plus Diffractometer with Cu K_α radiation. The quantitative phase analyses and the crystal structure parameters were analysed by the Rietveld method, refining the XRD patterns by GSAS code [20]. The hydrogen content and thermal stability were analysed and calculated by thermo-gravimetric (TG) analysis on a Netzsch simultaneous thermal analyser (STA), model 449 F3 Jupiter.

The MCE was quantified via the adiabatic temperature change, ΔT_{ad}, measured in different synthesised samples using a home-built ΔT_{ad}-ometer device [21]. In this device the sample is rapidly subjected to an applied magnetic field change from 0 to 1.75 T, starting from a stabilised sample temperature between 258 K and 348 K.

4

3. Results

In order to study the influence of the hydrogenation step on the amount of La(Fe,Si)$_{13}$ and on the lattice parameter a in the HDSH samples, XRD diffraction patterns were refined for both the samples before and after the hydrogenation processes as can be seen in Fig. 1(a). The amount of α-Fe increases with

the hydrogenation time, from 0.97 wt.% for the as-sintered sample to 2.92 wt.% and 6.13 wt.% for 2 h and 4 h of hydrogenation step, respectively, as shown in Fig. 1(b). The increase of α-Fe content could be related to formation of La oxide or LaH$_2$, which even in amounts undetectable by XRD, could lead to significant precipitation of α-Fe, as the structure La(Fe,Si)$_{13}$ is mostly Fe.

The lattice parameter a after the hydrogenation was increased from 11.48 Å to 11.59 Å, for both 2 h and 4 h of hydrogenation, which in the XRD data may be seen as a shift of the XRD pattern to lower angles, as shown in Fig. 1(b). These results are summarized in Table 1.
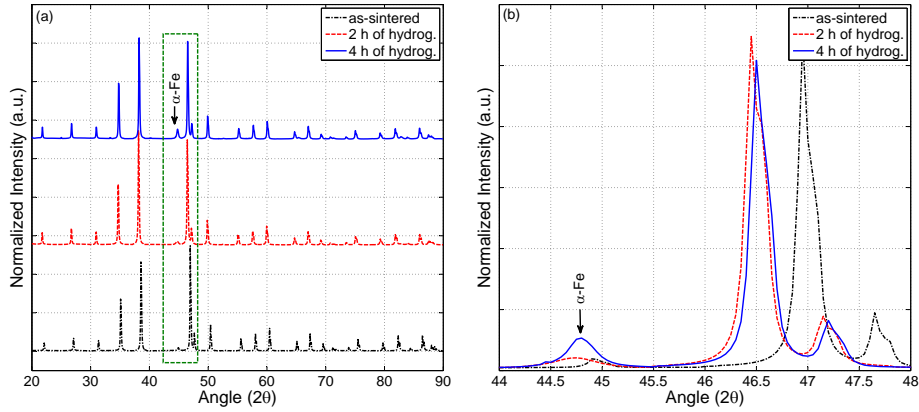

Figure 1: Colors are avaliable in online version. (a) Rietveld pattern for the XRD data of samples prepared by HDSH before hydrogenation (as-sintered), after 2 h (red line) and 4 h (blue line) of hydrogenation. (b) A zoom in the green dashed box from Fig.1(a) showing the shift on the pattern due to hydrogenation and the α-Fe peaks.

Thermal analyses of the hydrogenated samples were performed to understand the thermal stability of the interstitial hydrogen as a function of the tem-

5

perature. Fig. 2 summarizes the thermo-gravimetric analyses performed in the samples produced by HDSH compared to those produced by the conventional method. The thermal analyses shows two different H desorption ranges for the samples produced by HDSH, which may be related to a gradient of hydrogen, since these parts were hydrogenised in the bulk form. Also, as shown in Fig. 2, the gradient increases with the duration of the hydrogenation. Furthermore, these results indicate that the amount of interstitial H is higher for the parts produced by HDSH.

Although it is expected that longer hydrogenation times should lead to a lower H gradient [22], the different hydrogen contents might be related to the $\alpha-$Fe precipitation. When $\alpha-$Fe precipitates, the ratio $\alpha-$Fe/Si changes, hence changing the hydrogen saturation locally, which could lead to a greater gradient. Other relevant hydrogenation methods are found in the literature [13, 22], which might hydrogenate the sintered samples more efficiently.

Fig. 3 shows the ΔT_{ad} of the different samples with T_{C} around room temperature. it should be noted that the demagnetization factor, N_D, is different for each sample due to the differences in the shape between each sample. The N_D for the samples from the conventional process, HDSH with 2 h and 4 h of hydrogenation are 0.27, 0.32 and 0.49, respectively [23]. The temperature at which ΔT_{ad} is maximum, T_{peak}, was found to be around 329 K for the samples produced by the conventional process and by HDSH with 2 h of hydrogenation, while T_{peak} was 328 K for the sample produced by HDSH with 4 h of hydrogenation. The sample obtained by the conventional process and tested

Table 1: Relative phase amount and lattice parameter a, obtained by Rietveld refinement, of the samples produced by HDSH before the hydrogenation step (as-sintered), after 2 h and after 4 h of hydrogenation. The as-sintered sample measurements were taken before hydrogenation.

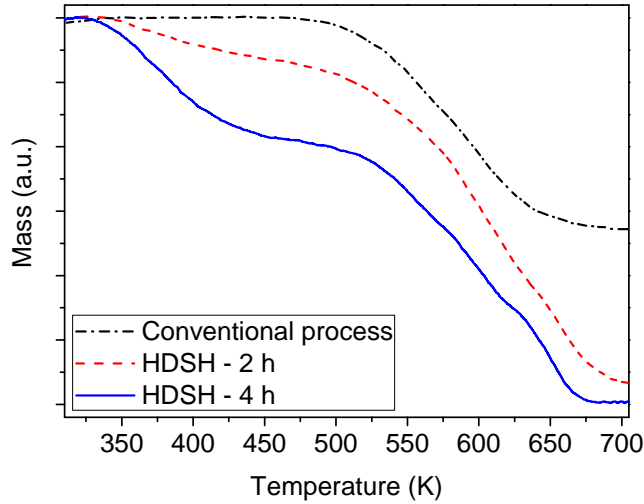| Description	a	$\mathbf{La(Fe,Si)_{13}H}y$	$\alpha-$Fe	LaFeSi
As-Sintered	11.48 Å	99.03 wt.%	0.97 wt.%	0.00 wt.%
HDSH (2 h)	11.59 Å	97.08 wt.%	2.92 wt.%	0.00 wt.%
HDSH (4 h)	11.59 Å	93.58 wt.%	6.13 wt.%	0.34 wt.%

6

Figure 2: Colors are avaliable in online version. Thermo-gravimetric analyses comparing the H desorption dependence on the temperature for the samples produced by the conventional method (black line) and HDSH with 2 h (red line) and 4 h (blue line) of hydrogenation.

in powder form still resulted in a larger ΔT_{ad}, with a maximum value of 2.64

120 K. The maximum values of the ΔT_{ad} for the bulk parts produced by HDSH process with 2 h and 4 h of hydrogenation were 2.07 K and 1.57 K, respectively. However, the parts produced by HDSH exhibited peaks that were broader than those produced by the conventional process. It is important to point out that the part hydrogenised for 4 h had a ΔT_{ad} larger than 1 K for a temperature

125 range of 40 K. These range differences can be also related to the H gradients which are observed in Fig. 2. The results are summarized in Table 2. Considering the broader MCE observed in the samples produced by HDSH, this process may be advantageous in the production of bulk materials for magnetic cooling devices, since fabrication of graded FOPT magnetocaloric materials is still in

130 development.

It should be noted that the measured MCE is influenced by the N_D of the samples, which reduces the resulting internal magnetic field. Therefore, the three curves should exhibit larger values of ΔT_{ad}. In this way, the samples produced by HDSH process should have maximum values of ΔT_{ad} closer to

that of the sample produced by the conventional process. Simple calculations based on the scaling relationship $\Delta T_{ad} \sim H^{2/3}$ show that the difference between the maximum value of ΔT_{ad} is significantly larger only for the sample produced by HDSH with 4 h of hydrogenation, as its N_D is 0.49.

A relationship has been identified between the reduction of the MCE and the phase content fraction as well. Firstly, due to $\alpha-$Fe precipitation, some distribution on x and y of $LaFe_{11.3-x}Si_{1.7+x}H_y$ may be found, instead of one singular value. For the 2 h hydrogenation HDSH sample, the total amount of $\alpha-$Fe was 2.92 wt.%, while for the 4 h hydrogenation HDSH sample the $\alpha-$Fe amount was 6.13 wt.%. The difference of α–Fe content, not only decreases the MCE due to the lower global amount of $La(Fe,Si)_{13}H_y$, but it may also create preferential pathways for the magnetic flux through the $\alpha-$Fe impurity grains rather than through the surrounding $La(Fe,Si)_{13}H_y$ matrix, because of the higher magnetic susceptibility of the former. A simple 2D magnetostatic model was set up to analyse the effect of the magnetic susceptibility. In the model a magnetic field is applied to rectangular sample with the susceptibility of $La(Fe,Si)_{13}H_y$, and the average internal field is calculated. Then areas equivalent to 2.92 and 6.13 wt.% of α–Fe were substituted as randomly positioned fine grains in the matrix of $La(Fe,Si)_{13}H_y$, equivalent to the samples produced by HDSH with 2 and 4 h of hydrogenation, respectively. In both situations the average internal field in the matrix around the α–Fe grains was observed to be within 1% of the value for the pure sample. Thus, the effect of the α–Fe impurities on the internal

Table 2: Summary of the ΔT_{ad} measurements. In this case, ΔT_{ad}^{Max} is the maximum value of ΔT_{ad} at T_{peak}.

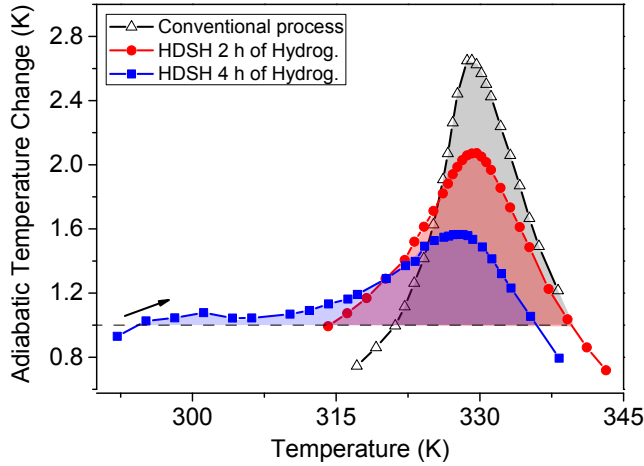| Sample	N_D	T_{peak}	ΔT_{ad}^{Max}	Range of $\Delta T_{ad} \geq 1$ K
Conventional	0.27	329 K	2.64 K	18 K
HDSH (2 h)	0.32	329 K	2.07 K	24 K
HDSH (4 h)	0.49	328 K	1.57 K	40 K

Figure 3: Colors are avaliable in online version. Adiabatic temperature changes, measured during heating and magnetization, for the La(Fe,Si)$_{13}$H$_y$ samples produced by the conventional process (black line), HDSH with 2 h (red line) and 4 h (blue line) of hydrogenation.

magnetic field is negligible.

4. Conclusions

In this paper, a comparison between the hydrogenation process of La(Fe,Si)$_{13}$H$_y$ compound in: i) powder and ii) sintered porous samples was carried out, from which the following conclusions could be withdrawn. Firstly, XRD patterns have shown an increasing intensity of α–Fe after the hydrogenation, in the case of samples prepared by HDSH. Thermal analysis revealed a gradient of H desorption ranges in the samples produced by HDSH. This gradient was also identified in the ΔT_{ad} measurements, where the sample produced by HDSH with 4 h of hydrogenation showed a ΔT_{ad} larger than 1 K in a range of 40 K. The maximum ΔT_{ad} of the samples produced by the conventional process, HDSH with 2 h and 4 h of hydrogenation were 2.64, 2.07 and 1.57, respectively. 2D modelling showed that the effect of $\alpha-$Fe on the surrounding magnetocaloric material is negligible.

9

5. Acknowledgements

References

[1] A. Smith, Who discovered the magnetocaloric effect?, The European Physical Journal H 38 (2013) 507–517.

[2] W. Giauque, D. Macdougall, Attainment of Temperatures Below 1 Absolute by Demagnetization of $Gd_2(SO_4)_3 8H_2O$, Physics Reviews 43 (9) (1933) 768.

[3] G. V. Brown, Magnetic heat pumping near room temperature, Journal of Applied Physics 47 (1976) 3673–3680.

[4] K. A. Gschneidner, Jr., V. K. Pcharsky, Thirty years of near room temperature magnetic cooling: Where we are today and future prospects, International Journal of Refrigeration 31 (2008) 945–961.

[5] J. A. Lozano, K. Engelbrecht, C. R. H. Bahl, K. K. Nielsen, D. Eriksen, U. L. Olsen, J. R. Barbosa Jr., A. Smith, A. T. Prata, N. Pryds, Performance analysis of a rotary active magnetic refrigerator, Applied Energy 111 (2013) 669–680.

[6] V. K. Pecharsky, K. A. Gschneidner, Jr., Giant Magnetocaloric Effect in $Gd_5Si_2Ge_2$, Physical Reviews Letters 78 (3) (1997) 4494–4497.

[7] A. Smith, C. R. H. Bahl, R. Bjork, K. Engelbrecht, K. K. Nielsen, N. Pryds, Materials Challenges for High Performance Magnetocaloric Refrigeration Devices, Advanced Energy Materials 2 (2012) 1288–1318.

[8] A. Fujita, A. Y., K. Fukachimi, Itinerant electron metamagnetic transition in $La(Fe_x,Si_{(1-x)})_{13}$ intermetallic compounds., Journal of applied Physics 85 (8) (1999) 4756–4758.

10

[9] F. Hu, B. Shen, J. Sun, Z. Cheng, G. Rao, X. Zhang, Influence of negative lattice expansion and metamagnetic transition on magnetic entropy change in the compound $LaFe_{11.4}Si_{1.6}$, Applied Physics Letters 78 (23) (2001) 3675–3677.

[10] J. Liu, M. Krautz, K. Skokov, T. G. Woodcock, O. Gutfleisch, Systematic study of the microstructure, entropy change and adiabatic temperature change in optimized LaFeSi alloys, Acta Materialia 59 (2011) 3602–3611.

[11] O. Gutfleisch, A. Yan, K.-H. Mller, Large magnetocaloric effect in melt-spun $LaFe_{13-x}Si_x$, Journal of Applied Physics 97 (2005) 10M305.

[12] B. R. Hansen, L. T. Kuhn, C. R. H. Bahl, M. Lundberg, C. Ancona-Torres, M. Katter, Properties of magnetocaloric $La(Fe,Co,Si)_{13}$ produced by powder metallurgy, Journal of Magnetism and Magnetic Materials 322 (2010) 3447–3454.

[13] C. S. Teixeira, L. Caron, A. Anastasopol, S. W. H. Eijt, J. A. Lozano, E. Brück, P. A. P. Wendhausen, A new feature of the reduction-diffusion process applied for the synthesis of magnetocaloric $LaFe_{13-x}Si_x$ compounds, Journal of Alloys and Compounds 541 (2012) 84–87.

[14] A. Fujita, S. Fujieda, K. Fukamichi, H. Mitamura, T. Goto, Itinerant-electron metamagnetic transition and large magnetovolume effects in $La(Fe_xSi_{1-x}$ compounds, Physical Review B 65 (2001) 014410.

[15] K. Fukamichi, A. Fujita, S. Fujieda, Large magnetocaloric effects and thermal transport properties of $La(FeSi)_{13}$ and their hydrides, Journal of Alloys and Compounds 408–412 (2006) 307–312.

[16] C. S. Teixeira, M. Krautz, J. D. Moore, K. Skokov, J. Liu, P. A. P. Wendhausen, O. Gutfleisch, Effect of carbon on magnetocaloric effect of $LaFe_{11.6}Si_{1.4}$ compounds and on the thermal stability of its hydrides, Journal of Applied Physics 111 (2012) 07A927.

11

[17] M. Krautz, J. D. Moore, K. P. Skokov, J. Liu, C. S. Teixeira, R. Schfer, L. Schultz, O. Gutfleisch, Reversible solid-state hydrogen-pump driven by magnetostructural transformation in the prototype system La(Fe,Si)$_{13}$H$_y$, Journal of Applied Physics 112 (2012) 083918.

[18] T. Numazawa, K. Mastumoto, Y. Yanagisawa, H. Nakagome, A modeling study on the geometry of active magnetic regenerator, Advanced Cryogenics Engineering 1434 (2012) 327–334.

[19] H. N. Bez, C. S. Teixeira, B. G. F. Eggert, J. A. Lozano, M. S. Capovilla, J. R. Barbosa Jr., P. A. P. Wendhausen, Synthesis of Room-Temperature Magnetic Refrigerants Based on La-Fe-Si by a Novel Process, IEEE Transactions on Magnetics 49 (8) (2013) 4626–4629.

[20] A. Larson, R. V. Dreele, General Structure Analysis System (GSAS), Tech. rep., Los Alamos National Laboratory (1994).

[21] P. V. Trevizoli, J. R. Barbosa Jr., P. A. Oliveira, F. C. Canesin, R. T. S. Ferreira, Assessment of demagnetization phenomena in the performance of an active magnetic regenerator, International Journal of Refrigeration 35 (2012) 1043–1054.

[22] J. Lyubina, U. Hannemann, M. P. Ryan, L. F. Cohen, Electrolytic hydriding of LaFe(13-x)Si(x) alloys for energy efficient magnetic cooling., Advanced materials (Deerfield Beach, Fla.) 24 (15) (2012) 2042–6.

[23] A. Aharoni, Demagnetizing factors for rectangular ferromagnetic prisms, Jounal of Applied Physics 83 (6) (1998) 3432–3434.